**ORIGINAL PAPER**

# Satellite-based analysis of the spatial patterns of fire- and storm-related forest disturbances in the Ural region, Russia

Andrey N. Shikhov[1] · Ekaterina S. Perminova[2] · Sergey I. Perminov[2]

## Abstract

Large-scale wildfires and windstorms are the most important disturbance agents for the Russian boreal forests. The paper presents an assessment of fire-related and wind-induced forest losses in the Ural region of Russia for 2000–2014. The assessment is based on the use of Landsat images, Global Forest Change dataset (Hansen et al. in Science 342:850–853, 2013. https://doi.org/10.1126/science.1244693) and other space imagery data. The total area of stand-replacement fires and windthrows in the Ural's forests was estimated at 1.637 million ha, which is 1.56% of the total forest-covered area. The contribution of wildfires and windthrows is 96.4% and 3.6%, respectively. The highest frequency of large-scale wildfires was observed behind the Northern Ural ridge, where the fire scars of 2000–2014 covered 10–14% of the forested area. The storm-related forest damage is significant only on the western part of the Ural. A few catastrophic wildfires and windthrows (with an area > 5000 ha) make up 35% of the entire damaged area. The number of wildfires, windthrows and their damaged area vary significantly from year to year. For 2000–2014, it is impossible to find a statistically significant trend of the fire- and storm-damaged area. The seasonal maximum of large-scale wildfires and windthrows was observed in July. Also, we identified the statistically significant relationships of fire- and wind-related forest damage with environmental variables. The occurrence of large-scale wildfires is related mainly to the species composition of forests, and also to the altitude, the mean annual precipitation and the population density. The spatial distribution of massive windthrows has a strong correlation with the species composition of forests, the mean annual precipitation and partially with the wind effect parameter.

**Keywords** Forest fires · Windthrows · Long-term data series · Spatio-temporal distribution · Global Forest Change data · Landsat images · Ural region

✉ Andrey N. Shikhov
  shikhovan@gmail.com

[1] Perm State University, Perm, Russia

[2] SCANEX Group, Moscow, Russia

# 1 Introduction

Fire- and wind-related forest cover disturbances are the most important natural factors determining the dynamics of boreal forest ecosystems (Seidl et al. 2011b). At the same time, the large-scale forest fires and windthrows can be natural disasters, which cause loss of life and considerable damage to many sectors of economy. Recently, fire- and wind-related forest damage has increased in many regions of the world, which can be associated with human-induced global warming (Seidl et al. 2011a, 2017). In particular, there is an increase in wildfires in Siberian boreal forests (Soja et al. 2007; Kukavskaya et al. 2016), and windthrows in Western, Central and Northern Europe (Seidl et al. 2011a, 2014; Gregow et al. 2017). It is considered that the observed increase in natural forest disturbances is one of the main environmental effects of the global warming (Seidl et al. 2011a).

The scenarios of climate change for the twenty-first century suggest a further increase in boreal forest damage caused by wildfires (Shuman et al. 2017) and windstorms (Seidl et al. 2014, 2017). The wildfires frequency and intensity may increase through the extension of the fire-hazard season, and also because of the blocking anticyclones and growing frequency of droughts (Eliseev et al. 2014). The amplification of storm-related damage can be associated with an intensification of the deep convection induced by the temperature rise in a warm season (Lassig and Moĉalov 2000; Schlyter et al. 2006; Diffenbaugh et al. 2013).

Boreal forests cover more than 40% of the territory of Russia. They have various disturbances regimes, which is formed by the stands' species composition and climatic features. For the entire territory of Russia, wildfires are responsible for about 65.5% of forest losses area, 30% is due by logging, and another 4.5% are related to windthrows, insect outbreaks and other drivers (Krylov et al. 2014). However, over 90% of large-scale wildfires occur in Siberia. In the European part of Russia, the contribution of wildfires to the total forest losses was estimated as only 8.1% for 1985–2012 (Potapov et al. 2015). In turn, large-scale windthrows happen more often in European Russia and induced 1.6% of total forest losses for 1985–2012 (Potapov et al. 2015). In 2007–2012, the contribution of fires and windthrows to the forest losses in the European Russia has increased to 11.3% (Potapov et al. 2015), which is due mainly to catastrophic wildfires in summer 2010 and large-scale windthrows of 2009–2010.

The Ural region, which forms the border between the European Russia and Siberia, is characterized by a high diversity of forest ecosystems and consequently by various regimes of forest disturbances. Boreal forests cover more than 45% of the Ural territory (Bartalev et al. 2004), and they are regularly exposed to extreme weather conditions, causing forest damage. The Eastern slope of the Ural Mountains has a much higher wildfire risk than the Western Ural, which is due to the differences in the precipitation amount. Groisman et al. (2007) noted that during the second half of the twentieth century, the wildfire risk (according to weather conditions) increased to the east of the Ural and decreased in the Western Ural.

The susceptibility of the Ural's forests to natural disturbances was studied even before the availability of long-term satellite imagery data. The first investigations were based on the analysis of literature review, field observations and aerial survey data. Lassig and Moĉalov (2000) studied the spatio-temporal distribution of large-scale windthrows in the Ural's forests for the period 1946–1995. Also, two catastrophic windthrow events of June 1975 in the Northern Ural and June 1995 in the Middle Ural

have been described by (Moĉalov 2002). After 2002, no one assessed the fire- and wind-related forest cover disturbances in the Ural region.

After the publication of the free-available Landsat archive (Wulder et al. 2012), a possibility of operational and reliable monitoring of wildfires and windthrows has been improved significantly. The satellite-based estimates of forest damage caused by wildfires (Bartalev et al. 2007; Loboda et al. 2007; Stytsenko et al. 2013) and severe storms (Krylov et al. 2012; Baumann et al. 2014) in Russia, including the Ural region, have become standard and widely used. Low-resolution satellite data such as Terra/Aqua MODIS and SPOT-Vegetation were mainly used to detect burned area for the entire Northern Eurasia (Egorov et al. 2008), and the identification of windthrows is based most often on the Landsat images with a 30-m spatial resolution (Koroleva and Ershov 2012; Krylov et al. 2012).

After the publication of the Global Forest Change (GFC) (Hansen et al. 2013) and Eastern Europe Forest Cover Change data (Potapov et al. 2015), there appeared new possibilities of the high-resolution analysis of long-term dynamics of forest disturbances, including fire- and storm-induced damage. Krylov et al. (2014) used the GFC data to study the spatial and temporal distribution of stand-replacement wildfires in Russia for 2002–2011, and estimated their total area as 17.6 million ha. Potapov et al. (2015) assessed the contribution of wildfires and windthrows to the forest losses in the Eastern Europe in 1985–2012 based on the full Landsat archive. These two studies provided an overall assessment of fire- and wind-related forest disturbances in Russia. A more detailed investigation, highlighting the regional features of natural forest cover disturbances, was carried out for the Russian European North (Potapov et al. 2012).

At the regional-scale level, it is important not only to create a long-term database of fire- and wind-related forest disturbances, but also to find the spatial patterns of wildfires and windthrows distribution. The identification of relationships between wildfires and windthrows occurrence (or their damaged area) and environmental variables, such as vegetation, topography, climate variables, human activity, can be used for GIS-based modeling of wildfires and windthrows risk (Díaz-Delgado et al. 2004; Chuvieco et al. 2010; Seidl et al. 2011b).

In this paper, we consider the spatio-temporal distribution of large-scale forest fires and windthrows in the Ural based on GFC data and other satellite images for 2001–2014. Our main aims in this study are (1) to assess the impact of wildfires and windthrows on the forest cover of the Ural region in a changing climate, and (2) to identify the main environmental variables, affecting the forests susceptibility to wildfires and windthrows.

The outline of the paper is as follows: Sect. 2 briefly describes the study area; Sect. 3 focuses on the development of the geodatabase of forest fires and windthrows; Sect. 4 presents the analysis of spatio-temporal distribution of wildfires and windthrows, and also the relationships between forest-damaged area and some environmental variables; Sect. 5 provides the main results of the study.

## 2 Study area

The study area includes the Ural Mountains, as well as adjoining plains. Its boundaries are the meridians 50° and 70°E and the Russian Federation state border. The Ural Mountains are located in the central part of the territory, and they have altitude ranges from 500 to 1895 m. The Ural ridge is divided into the Southern, Middle, Northern, Subpolar and Polar Ural, which differ significantly in climatic and landscapes features.

The western part of the study area belongs to the East European Plain, with altitude ranges from sea level to 450 m, and the eastern part is located on the West Siberian Plain, which has a relatively flat terrain with a 0–300 m elevation (Fig. 1a).

The Ural region is related to several climatic zones with high diversity of climatic conditions. Most of the study area has a temperate humid climate. The average July temperature varies from + 8 °C on the Arctic coast to + 23 °C near the southern border of the territory. The mean annual precipitation varies from 300 mm in the southeast to more than 1000 mm on the western slope of the Ural Mountains (National Atlas of Russia 2008; Afonin et al. 2008).

According to the map (Bartalev et al. 2004), forests cover 42% of the study area. The prevailing forest species composition is determined by the climatic conditions and the features of forest management. Old-growth dark-coniferous forests cover large areas on the western slope of the Northern Ural Mountains and the adjacent plain (Degteva et al. 2015). The northern part of the West Siberian plain is mainly covered by light-coniferous (pine and larch) forests and peat bogs. The secondary mixed and small-leaved forests, which have re-grown after logging, are the most widespread between 56° and 60°N. To the south of 56°N, forests are mainly replaced by agricultural lands (Fig. 1b).
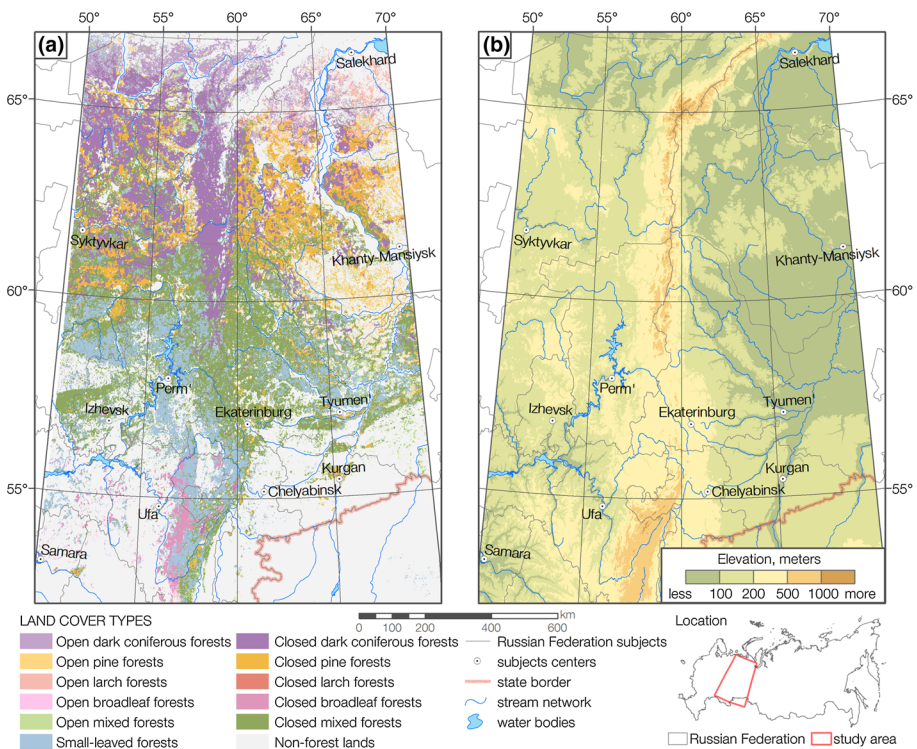


**Fig. 1** Vegetation types (**a**) and topography (**b**) of the study area

# 3 Geospatial datasets and methods

## 3.1 Data description

We have used the following data sources to create the database of fire-related and wind-induced forest cover disturbances in the Ural region:

- The 30 m-resolution Landsat-based Global Forest Change (GFC) map for the period 2001–2014 (Hansen et al. 2013). We used Forest Loss Year data to delineate forest cover disturbances. This dataset is provided as the integer raster with 30 m pixel size, containing information on the stand-replacement forest disturbances classified by years, without determining their causes. It was downloaded from (http://earthenginepartners.appspot.com/google.com/gMG7KbLG).
- The Collection 6 MODIS Active Fire data for 2001–2014 (Giglio et al. 2016), downloaded from (earthdata.nasa.gov/data/near-real-time-data/firms).
- The Map of Russian Forests (Dominating forest types and their canopy density, 1:14,000,000 scale) created by (Bartalev et al. 2004), downloaded from (http://terra norte.iki.rssi.ru/?).
- The Landsat Thematic Mapper (TM), Enhanced Thematic Mapper Plus (ETM+) and Operational Land Imager (OLI) images for 2000–2014, provided by the US Geological Survey (https://earthexplorer.usgs.gov/).
- The high-resolution (0.5–2 m) satellite images from public map services such as Google Maps, Bing Maps, HERE Maps, ESRI Imagery.

The identification and delineation of fire- and wind-related forest cover disturbances were performed based on the Forest Loss Year data (Hansen et al. 2013), using the ArcGIS 10.* software. The Python script was developed to automate the delineation process. The script allows you to select the pixels of the Forest Loss Year raster, containing the data on forest cover disturbances within a user-defined area and values interval, to perform a raster–vector transformation of the selected pixels and to write the data to the corresponding fields of attributive table. The type (fire- or wind-related damage) and data (or data ranges) were estimated for each identified disturbance. More detailed information on the delineation process is provided in Sects. 3.1 and 3.2.

Only stand-replacement disturbances have been considered in this study, because such disturbances may be detected by GFC data and Landsat images. According to Cohen et al. (2002), stand-replacement disturbances are characterized by substantial overstory tree mortality, observed immediately or during subsequent years after the impact of disturbance agents (clear-cut logging, wildfire or windstorm). Regarding wildfires, Krylov et al. (2014) noted, that the percentage of stand-replacement fires decreases along the North to South gradient from 50–60 to 10–20%. So, non-stand-replacement fires dominate in the Southern Ural (south of 56°N), while stand-replacement fires prevail in the north of 56°N. As for the wind-related disturbances, we have delineated only the areas with total or almost total removal of the canopy. Thus, the forest stands, slightly damaged by windstorms, are not considered in this study.

### 3.2 Assessment of fire-related forest disturbances

The identification of fire-related forest disturbances is based on the intersection of Landsat-based forest loss areas with MODIS active fire data. The forest disturbances, whose occurrence spatially and temporally coincided with MODIS-detected thermal anomalies (hot spots), have been identified as the fire-related losses (fire scars). It is important that the GFC data have relatively low time accuracy. Hansen et al. (2013) estimated that 24.8% of pixels of forest loss year data contain a ± 1 year error, and 3.3% of pixels possess a ± 2 year error due to the lack of cloud-free images. For instance, many of large fire scars associated with catastrophic fires in August 2010 were detected as forest losses occurred in 2011. Also, it is known that the post-fire tree mortality process can continue up to 5 years (Krylov et al. 2014). Therefore, all forest losses, occurring within 3 years after MODIS-detected fire events, have been considered as burned areas. The dates of fire occurrence were estimated by MODIS hot spots. If the fire was active during 2 months, we determined the month of fire occurrence by the date of its first detection.

The delineation of fire scars by the GFC data was performed semi-automatically using the Python script (see Sect. 3.1 for more details). Thus, we made the visual inspection of all fire-related forest disturbances, which allowed us to distinguish burned areas and neighboring man-made clear cutting.

De Groot et al. (2013) showed that 34% of all fires in Siberia are missed by the MODIS sensors, due to the fires being obscured by clouds and smoke, or not burning actively at the time of satellite overpass. This can lead to the underestimation of the fire-related forest losses. However, the scars of fires, which have not been detected by the MODIS sensors, may be identified by GFC data based on some geometrical features, e.g., an irregular shape of forest-damaged area. The analysis of the multi-temporal Landsat images allows you to find such forest disturbances and confirms that these are indeed fire scars. However, we cannot determine the dates when such fires were actively burning. For the period 2001–2014, we added 13.9 thous. ha of fires according to the GFC data and Landsat images, which were not previously detected by MODIS sensors. This is about 1% of the total burned area during 2001–2014, which is comparable with an assessment of Krylov et al. (2014), obtained for the entire Russia. The largest fire, which has not been detected by MODIS sensors, has an area of 793 ha.

Also we included in the analysis the fires of 2000, although the MODIS data are not available for this year. However, most of the forest cover disturbances occurred in 2000 have already been detected by GFC algorithm and are attributed as the forest losses of 2001. We have used the GFC data and multi-temporal Landsat-7 ETM + images, obtained in 1999 and 2000, to detect these fire scars. The main reason for considering the fires of 2000 in our analysis was the extreme fire-danger weather conditions observed in July 2000 on the Northern Ural. The total burned area in 2000 within the study area exceeded 327 thous. ha. Many uncontrolled forest fires happened in July 2000 in the Komi Republic (west of the Ural Ridge) and Khanty-Mansiysk autonomous region (east of the Ural ridge) (Potapov et al. 2012).

As a result, we included in our database 2080 forest fires with a total area of 1579 thousand ha. We excluded from the analysis all fires with burned area less than 25 ha. According to the classification of the Russian Federal Forestry Agency (Vorobiev et al. 2004), the fires with burned area exceeding 25 ha are classified as large fires in the European territory of Russia and the Ural region.

The accuracy of the obtained estimates of fire-related forest losses is determined by the spatial resolution of the Landsat images and GFC data, which is 30 m. In general, the use of GFC data deemed appropriate for regional-scale quantification of stand-replacement fires (Krylov et al. 2014). Hansen et al. (2013) estimated the overall accuracy of forest loss detection by the GFC data in the boreal zone as 99.3%, while the producer's accuracy is equal to 93.9%, the user's accuracy reaches 88.0%, and the mean omission error is equal to 6.1%. As for the assessment of burned area, the omission error may be slightly higher, than that for man-made forest losses. Krylov et al. (2014) showed that when estimating the burned area according to GFC data, the omission error (missed fire-related loss) exceeded the overestimation error (falsely attributed fire-related loss) by approximately 5 times. For the fires of 2000, the underestimation of the burned area may be somewhat higher, because of the lack of MODIS active fire data.

### 3.3 Assessment of storm- and tornado-induced forest disturbances

The identification of wind-related forest disturbances by the GFC data was performed based on their geometrical features. The great elongation coinciding with the wind direction and the linear or rambling spatial structure of forest-damaged areas are the main features of windthrows (Dyer 1988; Jedlovec et al. 2006; Krylov et al. 2012). The forest disturbances, classified as windthrows, were delineated by the GFC data. We excluded from the analysis the windthrows with an area less than 10 ha, since it is problematic to determine the dates of their occurrence and prove that these disturbances are really caused by windstorm (or tornado), and not by other drivers.

The visual verification was performed for each windthrow based on the high-resolution satellite images, obtained from public map services (Google Maps, Bing Maps, HERE Maps, ESRI). The main purpose of such verification was to determine the type of hazardous weather event (windstorm or tornado) causing forest disturbance. According to high-resolution images, we estimated the direction of the fallen trees, which made it possible to distinguish tornado-induced and windstorm-induced forest damage (Shikhov and Chernokulsky 2018). Tornado-induced windthrows are characterized by counterclockwise rotation of fallen trees (Bech et al. 2009). On the contrary, the direction of fallen trees in storm-induced windthrows generally coincides with the storm movement direction. Furthermore, the tornado tracks in forests are characterized by narrow and elongated geometry and mostly total removal of a canopy (Dyer 1988; Shikhov and Chernokulsky 2018), while the storm-induced windthrows often have a rambling spatial structure and various degrees of forest stand damage. The main features of windstorm- and tornado-induced forest disturbances are presented in Fig. 2.

The windthrows occurrence dates were determined using all available Landsat images and additional information sources. The analysis of multi-temporal Landsat images allows you to estimate the data range of storm events with an accuracy ranging from several days to 3 months (depending on the presence of cloudless images). The additional information, such as weather station reports, reanalysis data, eye-witnesses observations and media reports, was used to determine the exact dates of the events within the specified data range. For 74 windthrow events, we have determined the date of their occurrence with 1-day accuracy. On the other hand, the date of occurrence of 64 windthrows events was not determined even with one-month accuracy. In total, we have found and verified 92 storm-induced windthrows and 105 tornado-induced windthrows with an area of 49.1 thous. ha and of 10.8 thous. ha respectively.
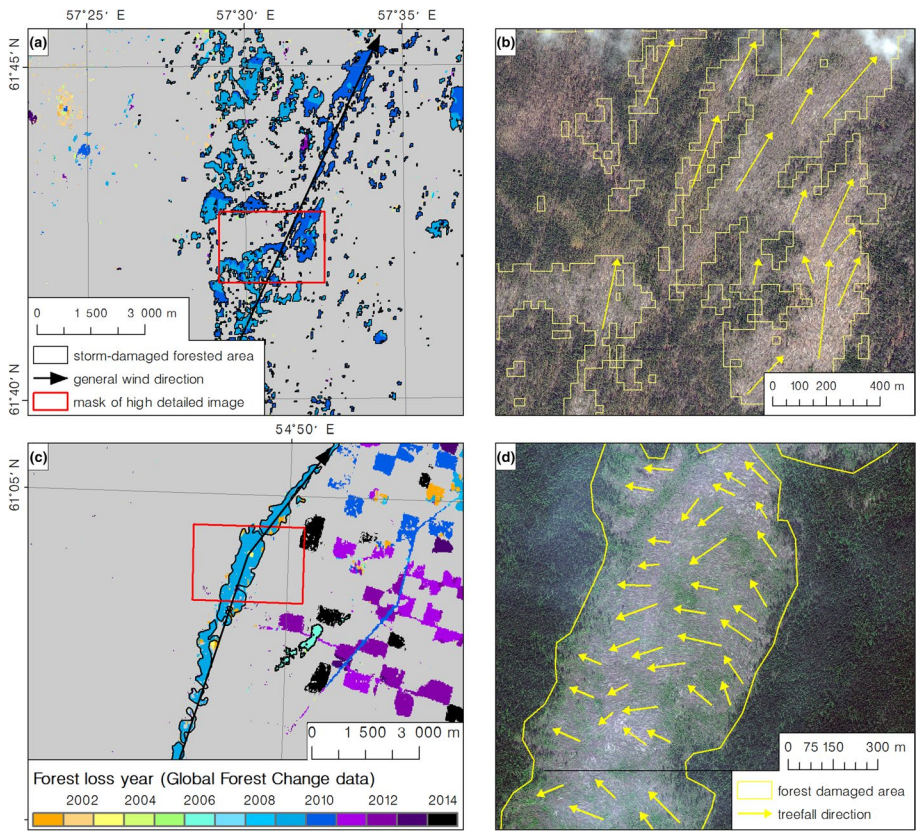
**Fig. 2** Features of forest disturbances due to windstorm (**a**, **b**) and tornado (**c**, **d**) occurred June 7, 2009, estimated using Global Forest Change map and high-resolution images

The accuracy of storm-related forest damage assessment is determined by GFC data reliability and spatial resolution. Koroleva and Ershov (2012), comparing the windthrow contours, detected by Landsat images and by high-resolution GeoEye images, found that the windthrows area can be estimated with 15% error if it exceed 2.6 ha. If the windthrow area is less than 2.6 ha, it will be significantly overestimated according to Landsat images. In the study area, some large windthrows consist of hundreds of small damaged areas, each of which is less than 2.6 hectares. So we may suppose that the area of such windthrows (which is 26% of total wind-damaged forested area) may be overestimated according to GFC data.

## 3.4 Analysis of the spatial patterns of forest damage distribution

### 3.4.1 Fire-related damage

Wildfires are the main driver of natural forest disturbances in Russia, including the Ural region (Krylov et al. 2014; Potapov et al. 2012, 2015; Shuman et al. 2017). So, the identification of spatial variables determining the forest susceptibility to stand-replacement

fires is a priority of our study. We used the overlay GIS analysis to identify the main spatial patterns of fire-affected area distribution. Díaz-Delgado et al. (2004) used the similar approach to estimate the spatial patterns of forest fires distribution in Catalonia. The area of fire scars was considered as dependent variables, and some environmental characteristics, related to fire occurrence, such as vegetation types, topography, climatic parameters and population density, were considered as the independent variables. Continuous variables such as altitude, temperature or precipitation, were converted in a categorical rank before the spatial overlay. Then, we calculated a percentage of the total burned area versus the total available surface covered by every class of the following independent variables:

*Forest vegetation types* were determined by Russia's Forest Map (Bartalev et al. 2004, Fig. 1a). The forest species composition is the main factor determining the fire regime and fire-affected area. The percentage of fire-affected area varies by 10 times or more within different forest types (Table 1). So, we subdivided the fire scars related to the different forest types (dark-coniferous, pine, larch, mixed and small-leaved forests) into separate datasets. Then, we estimated the relationships between the fire-damaged area and other environmental variables separately for each forest type.

*Topography (altitude, slope and slope aspect)* was estimated by Global Multi-resolution Terrain Elevation Data (GMTED-2010) with a 250-m spatial resolution, downloaded from USGS (https://earthexplorer.usgs.gov). Before you perform the spatial overlay with fire scars, these variables were converted in a categorical rank. Digital Elevation Model (DEM) was classified into 12 classes with a 50-m altitude step, and slope aspect was classified into 8 rhumbs. The slope raster was excluded from the analysis, since it has a high linear correlation with DEM (Pearson correlation coefficient is equal 0.6).

*Climatic variables:* We considered mean July temperature and mean annual precipitations as the climatic variables relevant to the fire occurrence. The climatic data with 1-km spatial resolution were downloaded from WorldClim 2.0 (http://worldclim.org/version2, Fick and Hijmans 2017). The climatic variables are continuous, so they were converted (reclassified) in a categorical rank.

**Table 1** Fire- and wind-damaged area for different land-cover types, estimated by Russia's dominating forest types map (Bartalev et al. 2004)

| Land-cover type | Area (km$^2$) | Burned area (km$^2$/%) | Wind-damaged area (km$^2$/%) |
| --- | --- | --- | --- |
| Non-forest lands | 1,377,060 | 2529.1/0.18 | – |
| Open dark-coniferous forests | 64,708 | 1204.6/1.86 | 2.5/0.004 |
| Open pine forests | 42,012 | 1032.8/2.46 | 1.0/0.002 |
| Open larch forests | 18,614 | 698.7/3.75 | 0/0 |
| Open broadleaf forests | 7165 | 0/0 | 0/0 |
| Open mixed forests | 70,792 | 361.9/0.51 | 5.6/0.008 |
| Closed dark-coniferous forests | 166,272 | 3094.1/1.86 | 213.6/0.128 |
| Closed pine forests | 118,931 | 3722.4/3.13 | 70.0/0.059 |
| Closed larch forests | 5362 | 365.0/6.81 | 0/0 |
| Closed broadleaf forests | 18,405 | 1.4/0.01 | 0/0 |
| Closed mixed forests | 294,431 | 2451.2/0.83 | 221.2/0.075 |
| Birch and aspen forests | 198,375 | 299.3/0.15 | 46.5/0.023 |

*Lightning frequency* was estimated by World Wide Lightning Location Network (WWLLN) data for the period 2008–2011. We used the global lightning climatology data with 1° spatial resolution (Virts et al. 2013).

*Rural population density* was estimated according to (National Atlas of Russia 2008).

### 3.4.2 Wind-related damage

The highest frequency of windthrows is known to be observed in the areas of low stand stability and/or high wind exposure (Gardiner et al. 2008; Seidl et al. 2011b). So, forest stand parameters (species composition, trees height, age and density) and topography are two main factors determining their susceptibility to windthrows. Precipitation amount and soil moisture also have a significant effect on the frequency of windthrows occurrence (Panferov et al. 2009). Within the study area, the forests susceptibility to windthrows is mainly determined by their species composition (Table 1). More than 75% of windthrows areas are related to two forest types, such as closed dark-coniferous and mixed forests. As for other forest stand parameters, such as trees height, age and stands density, we do not have the reliable data to evaluate them for the entire study area.

We have considered three environmental variables influencing the forest susceptibility to windthrows, such as vegetation types, mean annual precipitations and wind effect factor. The first two variables have been described above. The wind effect factor was calculated based on DEM and wind direction (degree), with the use of SAGA GIS v 2.3. (http://saga.sourcearchive.com/documentation/2.0.7plus-pdfsg-2/wind__effect_8cpp_source.html). When calculating wind effect, we estimated the typical wind direction for storms, causing windthrows (weighted by the damaged area). The wind directions from south to north and from southwest to northeast are typical for windthrow-induced storms. Since the wind effect is a continuous variable, the raster was converted in the categorical rank before the spatial overlay with wind-damaged areas.

## 4 Results and discussion

### 4.1 Spatial distribution of fire- and wind-related forest disturbances

The spatial distribution of wildfires and windthrows within the Ural region is characterized by strong unevenness (Fig. 3). Windthrows happen rarely in the areas with high wildfires frequency, and vice versa, areas with high windthrows frequency are characterized by low forest-fires recurrence. More than 90% of large wildfires occurred to the east of the Ural ridge, and most of large windthrows happened in the western part of the region. These patterns are mainly due to the forests species composition (Fig. 1a) and climatic features.

The maximum frequency of large wildfires in 2000–2014 was observed near the border of the Khanty-Mansiysk and Yamalo-Nenets autonomous districts, between 64° and 65°N, 63° and 68°E, where the fire scars cover 10–14% of the total forested area. The second maximum of large wildfires occurrence, with 10% of burned area, is located to the east of the Northern Ural ridge, near 61°N, 61°E. The maximum windthrows frequency has been observed to the west of the Ural Mountains, between 59° и 64°N, 54° и 59°E. Wind-induced forest disturbances cover there 0.5–2% of the entire forested area. The southwestern part of the Ural is characterized by very low frequency of large wildfires and
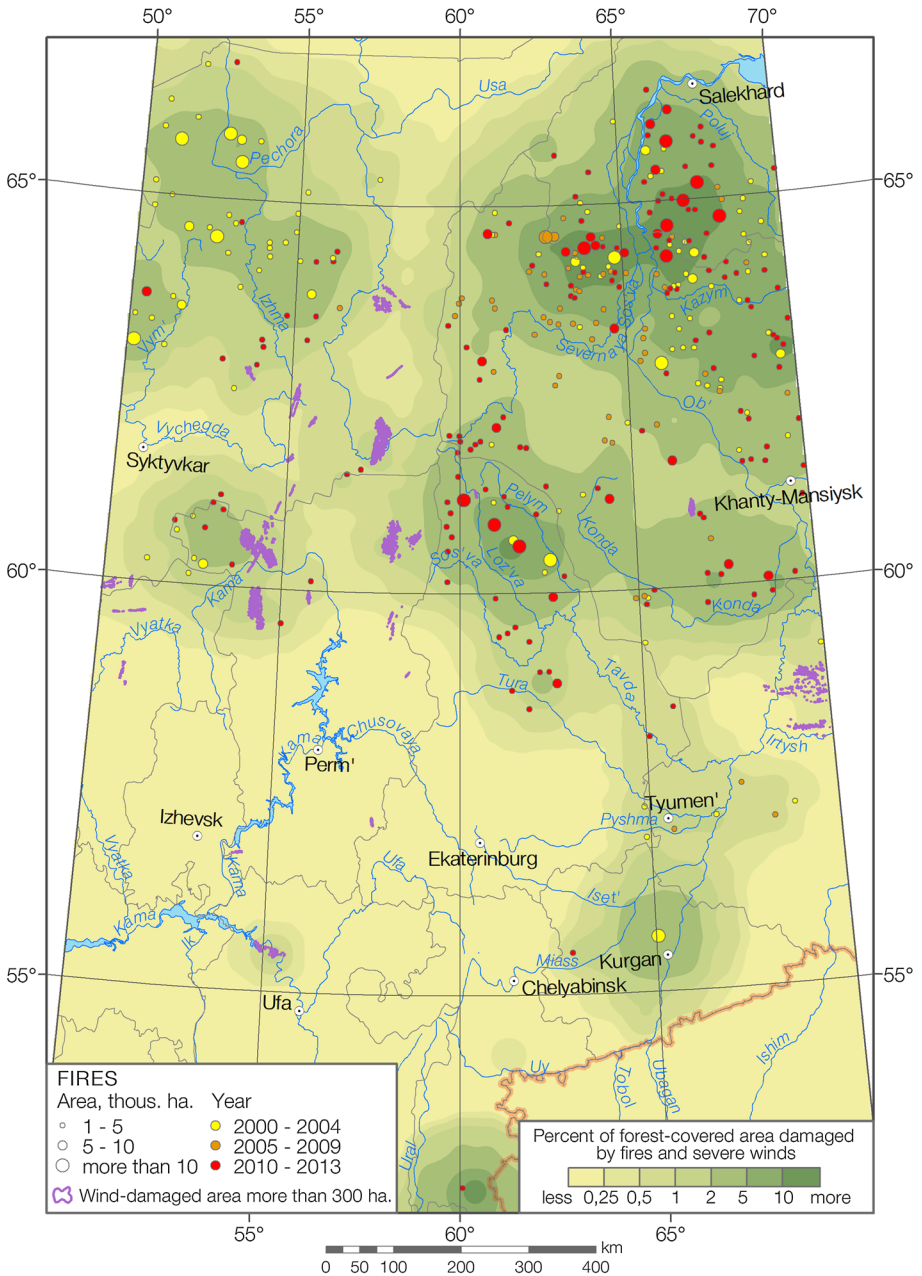
**Fig. 3** The spatial distribution of large fire-related and wind-induced forest disturbances between 2000 and 2014

windthrows. The fire- and wind-related forest disturbances cover there from 0.001 to 0.1% of the forested area.

Pine and larch forests, which are widespread mainly to the east of the Ural ridge, have highest susceptibility to wildfires (Table 1). From 2 to 14% of light-coniferous forests burned out in 2000–2014. West to the Ural ridge, the pine forests are also characterized by high frequency of large wildfires. The susceptibility of dark-coniferous and mixed forests to wildfires is significantly lower. However, in the extreme fire–weather conditions, such as the summers 2000 or 2010, the large uncontrolled fires may even occur in such forest types. The total fire-damaged area in dark-coniferous and mixed forests exceeds 550 thous. ha. The fire susceptibility of mountain forests is significantly lower than that of the plain ones.

On the other hand, the dark-coniferous and mixed forests are highly susceptible to windthrows (Table 1). The highest windthrows frequency has been observed in the mature dark-coniferous forests neighboring with logging. For example, the catastrophic windthrows observed on July 18, 2012, caused the largest damage in the areas of industrial logging.

## 4.2 Fires and windthrow size distribution

The total area of fire- and wind-related forest disturbances within the Ural region for 2000–2014 reached 1.637 million ha (1.56% of entire forest-covered area). The contribution of wildfires and windthrows is 96.4% and 3.6%, respectively.

The average and median size of stand-replacement fires is 759 ha and 196 ha, respectively (note, that only fires with an area exceeding 25 ha were included in the analysis). The largest wildfire happened in August 2010 near the eastern slope of the Northern Ural and burned 65.574 ha of forest. In addition to this largest fire, another 19 fires have an area exceeding 10 thousand ha.

The average and median size of stand-replacement windthrows is 302 ha and 51 ha, respectively, which is significantly lower than the same of wildfires. The largest windthrow happened on July 18, 2012, on the western slope of the Northern Ural and damaged 8.593 ha of forest. Also two wind-induced forest disturbances, occurred on July 18, 2012, and June 7, 2009, have an area exceeding 5000 ha.

We used the Lorenz curve to analyze the fires and windthrows size distribution, and calculated the Gini coefficient to estimate their inequality (Fig. 4). The Gini coefficient
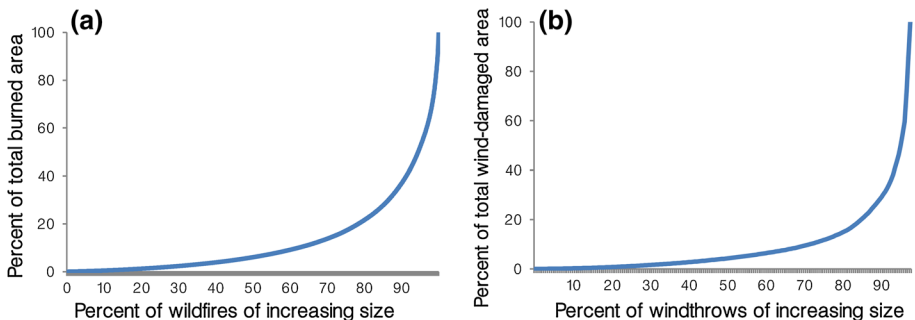


**Fig. 4** Lorenz curves of fire (**a**) and windthrow (**b**) size distribution in the Ural region, 2000–2014

for fires and windthrows distribution is 0.807 and 0.801, respectively. Such values show a strong inequality of the fire and windthrows size distribution. Indeed, most of the forest damage is associated with a relatively small number of large (catastrophic) events, while a large number of small disturbances do not cause significant damage. Fire size frequency distributions at 5-year intervals indicated that this inequality may increase during an extreme fire season. The Gini coefficient reached the highest value in 2010–2014, when the most severe droughts and largest wildfires had occurred.

### 4.3 Temporal distribution of the large forest fires and windthrows

#### 4.3.1 Inter-annual variability

The number of large wildfires and their area has strong inter-annual fluctuations. So, it is impossible to find a statistically significant trend for 2000–2014. The inter-annual distribution of forest fires has an evident cyclic recurrence (Fig. 5a). So, during 2006–2009, there a high precipitation amount was observed in summer, and large wildfires occurred rarely. Then, four dry and hot summer seasons with numerous wildfires occurred in 2010–2013. The most strong droughts and large-scale wildfires happened in 2010 and 2013, when the total burned area exceeded 300 thous. ha. In 2014–2015, the number of wildfires again decreased significantly, due to heavy rainfall and low air temperature in summer.

Note that these cycles are not identified across the entire Ural region. For example, in 2000, 2010 and 2013 the extreme wildfire–weather conditions and large forest fires were observed in different parts of the Ural. In total, six large wildfire outbreaks occurred during 2000–2014 (Table 2). Within the most fire-affected region, located near the Ob' river between 62° and 65°N, 62° and 68°E, large wildfire outbreaks occurred four times (in 2000, 2004, 2005 and 2013).

The inter-annual distribution of windthrows is determined by a few severe storms and tornadoes causing the largest forest damage. The most severe storms and tornadoes in the Ural region occurred in 2007, 2009, 2010 and 2012 (Table 3). Almost 80% of the total wind-related forest damage is associated with them. Between 2000 and 2006, there were no large windthrows within the study area. So, we can suppose that there is the significant increase in the windthrows frequency and wind-damaged area in the Ural region. A similar trend was found for the entire European Russia (Potapov et al. 2015).
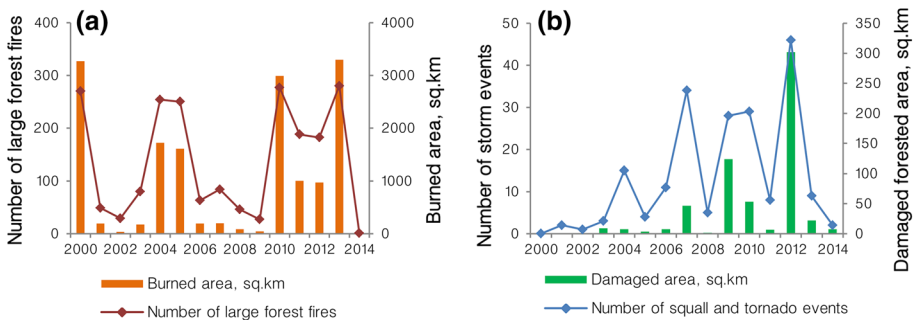


**Fig. 5** Inter-annual variability of forest fires and burned forested area (a); and squall and tornado events and wind-damaged forested area (b)

**Table 2** The most significant outbreaks of large wildfires in the Ural region between 2000 and 2014

| Dates (time period) | Fire-damaged area | Number of large wildfires and fire-damaged area (km²) | Wildfire–weather conditions characteristics |
|---|---|---|---|
| 15–30 July 2000 | The northern and northwestern part of the study area between 62° and 66°N, 50° and 70°E, within the Komi Republic and Khanty-Mansiysk autonomous region | 270 (327) | The long-lived blocking anticyclone settled over the northern part of the Ural region and caused hot and dry weather between July 10 and July 25, 2000. The air temperature reached +29…+34 °C during 15 day |
| 11–18 May 2004 | Southeastern part of the study area (near 56° N, 65° E), within the Kurgan and Tyumen' regions | 29 (375) | The advection of tropical air masses from Central Asia caused extreme wildfire–weather conditions with the air temperature increasing to +33…+36 °C and wind speed up to 20 m/s |
| 1 July 2004–8 Aug 2004 | The area located east of the Ural ridge, between 60° and 62°N, 60° and 62°E, within the northern part of the Sverdlovsk region | 160 (121) | The long-lived blocking anticyclone settled over the Northern Ural region due to hot and dry weather with the air temperature increase up to +30…+35 °C, during July 2004 |
| 23 July 2005–8 Aug 2005 | The area located near the Ob' river, between 63° and 65°N, 63° and 66°E, within the Khanty-Mansiysk Autonomous region | 220 (154) | The blocking anticyclone settled over the northern part of the Western-Siberian plain, caused hot and dry weather between July 23 and July 30, 2005, with air temperature up to +30…+33 °C |
| 24 July 2010–23 Aug 2010 | Northern Ural and adjoining plains, located between 59° and 63°N, 52° and 63°E, within the Perm and Sverdlovsk regions | 270 (299) | Extreme wildfire–weather conditions with the air temperature up to +30…+37 °C were observed under the influence of long-lived blocking anticyclone settled over European Russia and Ural (summer 2020 heat wave) |
| 20 July 2013–10 Aug 2013 | Area located near the Ob' river, between 63° and 66°N, 63° and 68°E, within the Khanty-Mansiysk and Yamalo-Nenets Autonomous regions | 150 (284) | The long-lived blocking anticyclone settled over the Yamal peninsula and caused extreme heat wave with the air temperature up to +30…+34 °C, between July 18 and August 10, 2013 |

**Table 3** The most severe windstorm and tornado outbreaks causing significant forest damage in the Ural region between 2000 and 2014

| Date | The storm-affected region | Forest-damaged area (ha) | Short characteristics of the storm event |
|---|---|---|---|
| 01 June 2007 | The northern part of the Bashkortostan Republic, near 56°N, 55°E | 2.329 | Severe convective storm with 30 m/s wind gusts, reported by Birsk weather station |
| 23 June 2007 | Eastern slope of the Northern Ural, between 60° and 64°N, 59° and 62°E, within the Sverdlovsk region and Khanty-Mansiysk Autonomous region | 1.420 | Tornado outbreak (more than 10 tornadoes) and strong downburst (38 m/s) reported by Burmantovo weather station |
| 07 June 2009 | The northern part of the Perm region and southeastern part of the Komi Republic between 59° and 62°N, 53° and 57°E | 10.600 | Tornado outbreak (more than 10 tornadoes) and strong downbursts which were not reported by the weather stations |
| 14 June 2010 | Tyumen' region, between 58° and 59°N, 68° and 70°N | 2500 | Severe convective storm with wind gusts more than 25 m/s |
| 11 Aug 2010 | The eastern part of the Komi Republic, near 64°N, 57°E | 1.840 | Severe convective storm, which was not reported by the weather stations |
| 18 July 2012 | The western slope of Northern Ural and adjoining lowland territory located between 59° and 61°N, 53° and 59°E, within the Perm region | 26,650 | Severe convective storm with maximum measured wind speed up to 28 m/s, severe downbursts and two tornado events |
| 17 June 2013 | North of the Kirov region, near 60°N, 51°E | 1465 | Strong tornado with path length up to 50 km and path width 500–1500 m |
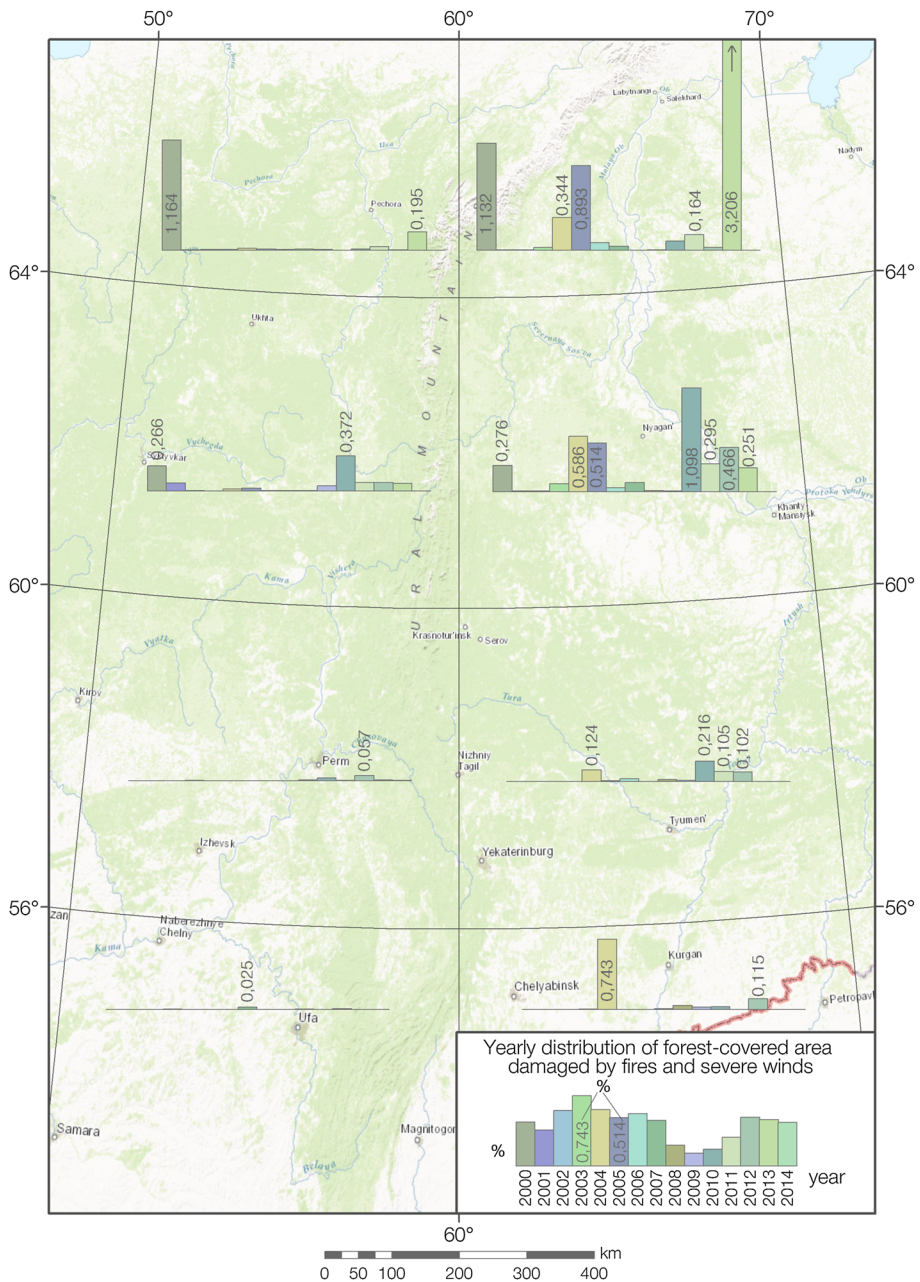
**Fig. 6** Inter-annual variability of fire- and wind-related forest cover losses in the Ural region in 2000–2014, within 4°×10° grid cells

Figure 6 shows the spatial heterogeneity of the inter-annual distribution of fire- and wind-related forest disturbances within the Ural region. The percentage of the forested area, affected by stand-replacement fires and windthrows, was calculated in 4°×10° grid

cells. This grid corresponds to the frequently used subdivision of the territory into the Southern, Middle, Northern and Subpolar Ural, as well as the Western and Eastern Ural.

The inter-annual variability of the forest-damaged area is mainly determined by wildfire–weather conditions during summer seasons. The most large forest damage was identified in 2000, 2004, 2005, 2010 and 2013, when the large wildfire outbreaks occurred. In the grid cell located between 56–60°N and 50–60°E, the largest forest losses were observed in 2012, due to the catastrophic windthrow on July 18, 2012. The southwestern cell is characterized by minor forest damage for the entire period, except 2007. The large-scale forest losses in 2007 were associated with the devastating storm on June 1, 2007, in Northern Bashkortostan (Dmitrieva and Peskov 2016), damaging over 2300 ha of forest.

### 4.3.2 Monthly distribution

The monthly distribution of large wildfires and windthrows is shown in Fig. 7. Most of the large wildfires occurred in the second half of July or early August. In June, the number of fires and their area is significantly lower due to the higher humidity of forest fuel after spring snowmelt. In 2004 and 2011, the large forest fires also occurred in May, when extreme fire–weather conditions (high air temperature, strong wind and very low relative humidity) were observed.

Most of the windthrow events occur in June, which corresponds to the seasonal maximum of strong convective storms and tornadoes frequency (Groenemeijer and Kuhne 2014). However, the largest windthrow happened on July 18, 2012; therefore, the maximum of wind-damaged area has shifted to July (Fig. 7b). We have not determined the month of the occurrence of 64 windthrow events; however, almost all these windthrows are relatively small in area. They occurred mainly in 2003–2006, when the frequency of the obtained Landsat images was lower than that in previous and subsequent years (Potapov et al. 2015).

### 4.4 Spatial patterns of the distribution of fire-related forest disturbances

### 4.4.1 Topographic variables

*Altitude* The inverse correlation between the fire-affected area and the altitude has been found for all forest types, with the Pearson coefficient ($R$) ranges from $-0.60$ to $-0.91$. This is due to the temperature decrease and precipitation increase in the mountains, which
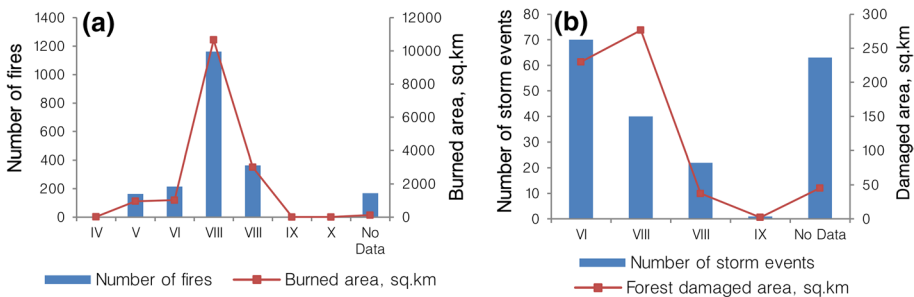


**Fig. 7** Monthly distribution of wildfires and burned area (**a**); and windthrows events and their area (**b**)
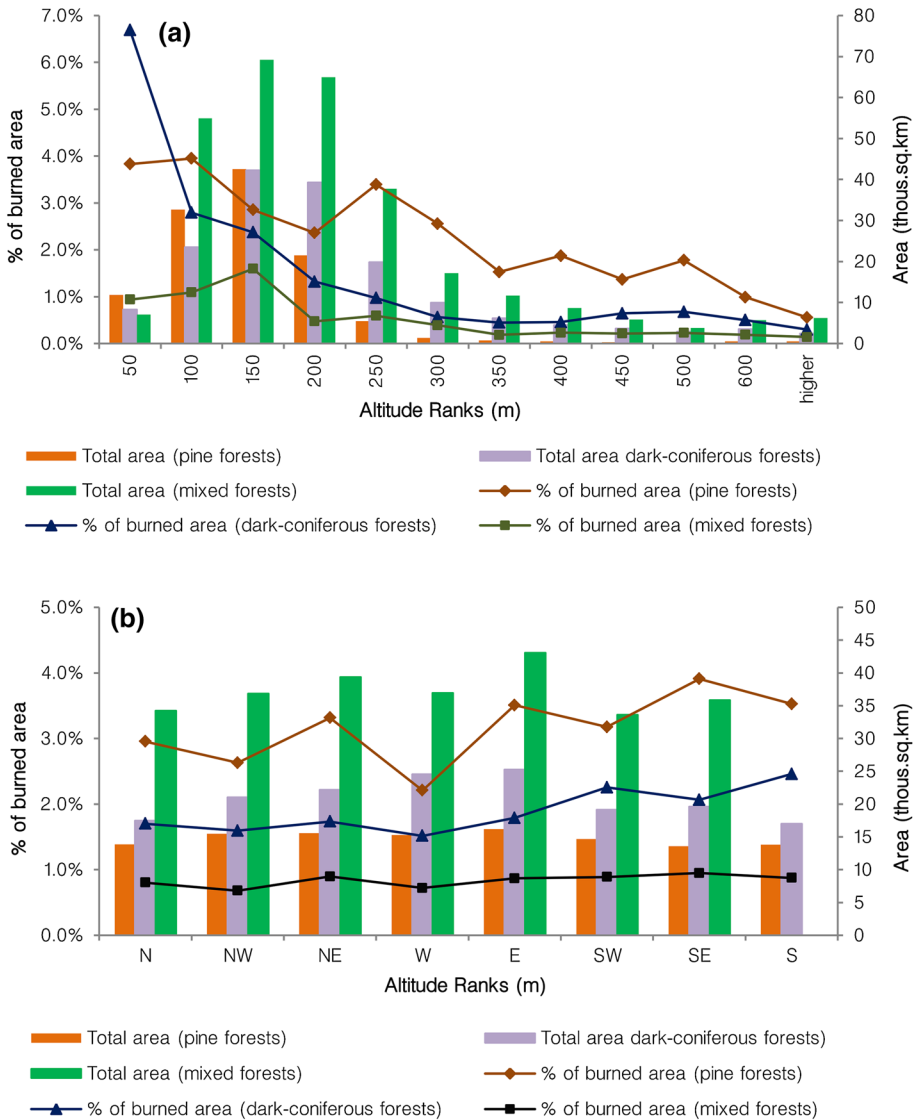
**Fig. 8** Percentage of burned area versus (**a**) altitude, (**b**) aspect. Bars indicate the proportion of every variable rank in the studied area, and lines show the percentage of burned area

leads to the decline of the frequency of wildfires occurrence. Figure 8a shows that the fire-affected area will reduce by 2–10 times (depending on the forest type) if the altitude exceeds 500 m. The correlation is strongest for dark-coniferous forests. In general, wildfires in the Ural Mountains at an altitude more than 500 m are infrequent, only the extreme fire season 2010 was an exception.

*Slope aspect* The correlation of the fire-affected area with a slope aspect is somewhat weaker than the same with an altitude, but it is also statistically significant, with $R$ ranges from 0.5 to 0.8 for the different forest types. The wildfires are known to occur most often on the southern slopes (Díaz-Delgado et al. 2004). In the Ural region, the southern and southeastern slopes are mostly affected by wildfires, and the well-moistened northwestern and western slopes have minimal fire susceptibility. In the pine forests, the fire-affected area ranges from 2.2% on the western slopes to 3.9% on the southeastern slopes. In the dark-coniferous forests, it ranges from 1.5% on the western slopes to 2.5% on the southern slopes. However, in the mixed forests this correlation is weak (Fig. 8b).

### 4.4.2 Climatic variables

*Mean July temperature* Contrary to possible assumptions, the correlation of the fire-damaged area with mean July temperature is not significant ($R < 0.45$), since large uncontrolled wildfires occur mainly in the northeastern part of the Ural. The mostly fire-affected area is located near 65°N (Fig. 2), where the average July temperature does not exceed 16 °C. To the south, the air temperature rises, but the fire-damaged area declines because of the change in forest species composition and growth of the population density. Only pine forests are an exception. They are highly susceptible to large wildfires in the southern parts of the study area, such as Kurgan region (Fig. 9a).

*Mean annual precipitation* Precipitation amount has a strong influence on the wildfire frequency and fire-damaged area. The inverse relationship between the burned area and mean annual precipitation is significant for all forest types, especially for dark-coniferous forests ($R = -0.89$). Indeed, behind the northern Ural ridge, where the wildfires have damaged the largest area of dark-coniferous forests, the mean annual precipitation is about 500 mm. On the western slope, the annual precipitation amount reaches 900 mm, and the burned area reduces significantly (Fig. 9b). For the pine forests, the correlation between burned area and mean annual precipitation is substantially weaker ($R = -0.55$). Thus, pine forests remain susceptible to wildfires even if the annual precipitation exceeds 700 mm. However, in the southeast of the Ural, where the precipitations amount does not exceed 500 mm, the fire scars in pine forests reach 7.5% of their total area.

*Lightning frequency* Thunderstorms are one of the main sources of forest fires, primarily in remote areas with low population density (Baranovskiy et al. 2016). However, the WWLLN-estimated lightning frequency (Virts et al. 2013) has a moderate negative correlation with wildfire frequency and fire-damaged area, with $R$ ranges from $-0.56$ to $-0.75$ for different forest types. The negative correlation is due to the maximum lightning frequency is observed in the areas with high precipitation amount (i.e., on the western slope of the Ural). On the eastern slope of the Ural, lightning frequency is much lower.

### 4.4.3 Rural population density

The population density has an ambiguous effect on the wildfires distribution. On the one hand, most of the wildfires have anthropogenic causes. On the other hand, wildfires can spread spontaneously and burn large areas in low-populated regions. In the Ural, the large fires occur mainly in the northern low-populated regions. So, there is a good inverse correlation between the fire-affected area and the population density (Fig. 10). Only pine forests
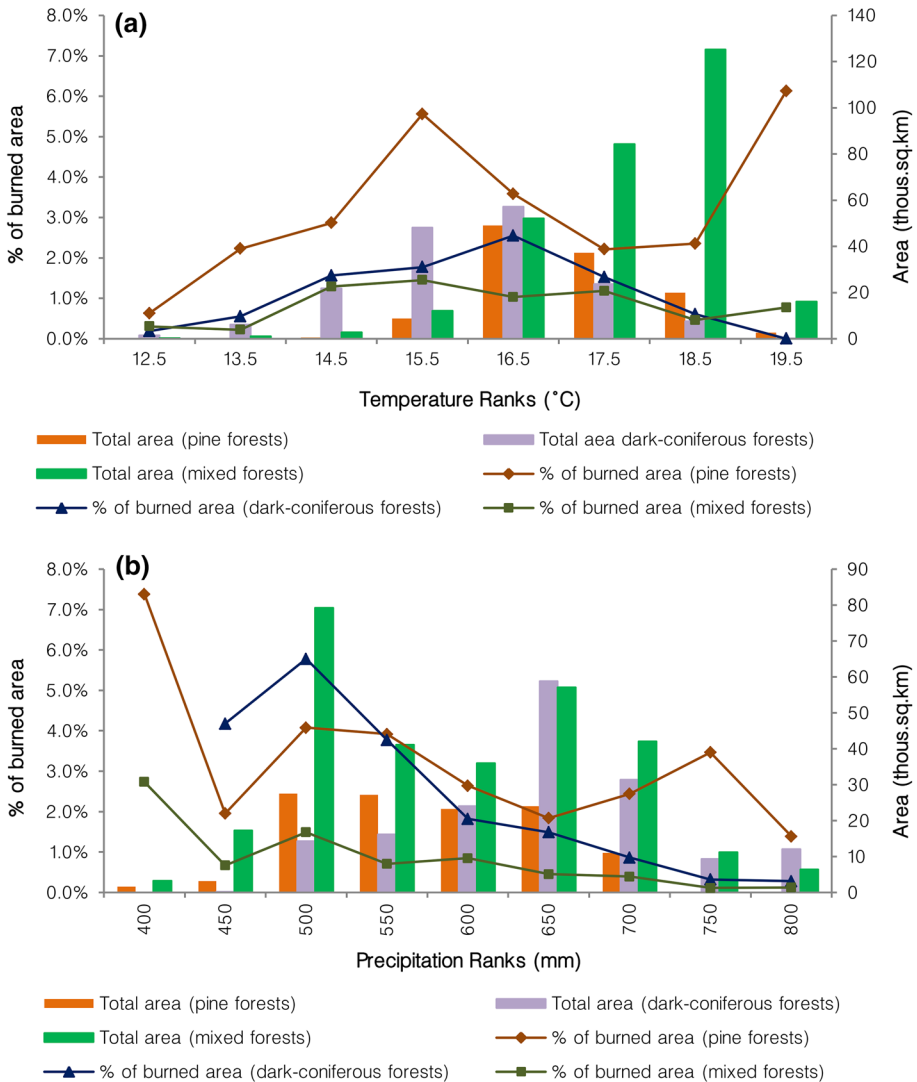
**Fig. 9** Percentage of burned area versus (**a**) mean July temperature, (**b**) mean annual precipitation. Bars indicate the proportion of every variable rank in the studied area, and lines show the percent of burned area

are an exception, because they are highly susceptible to wildfires even in high-populated areas (for example, in the Kurgan region). Such large and uncontrolled wildfires occurred in Kurgan region in May 2004 (see Table 2 for more details). They caused considerable damage and loss of life (http://eng.ntsomz.ru/projects/emergency/pojari_may).

## 4.5 Spatial patterns of the distribution of windthrows

*Annual precipitation* There is a moderate correlation ($R=0.6$) between mean annual precipitation and windthrows occurrence in dark-coniferous and mixed forests. The
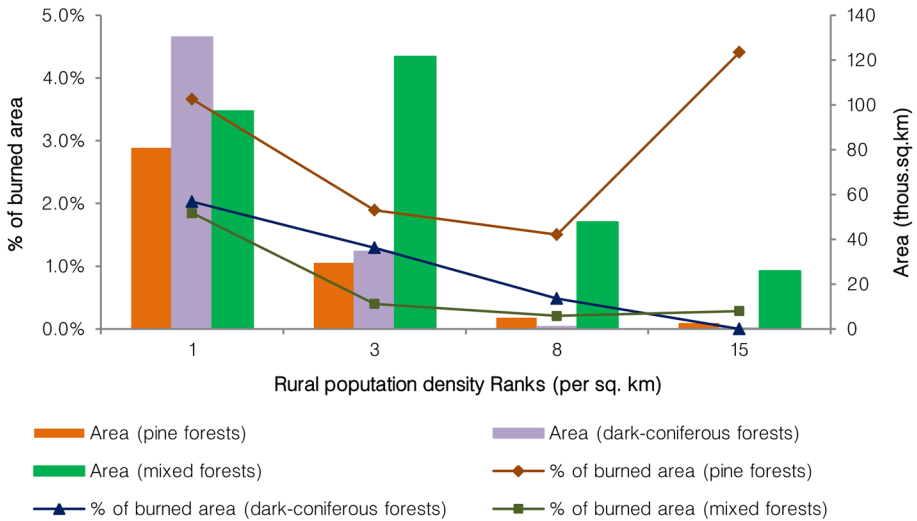
**Fig. 10** Percentage of burned area versus rural population density. Bars indicate the proportion of population density in the studied area, and lines show the percent of burned area

largest wind-induced forest damage is identified in the areas where the annual precipitation exceeds 700 mm (Fig. 11a). This correlation may be explained by the fact that the precipitation amount and soil moisture have a significant influence on the resistance of trees to the effects of strong wind (Panferov et al. 2009). In addition, weather conditions favorable for strong downbursts and tornadoes formation occur more often on the windward and well-moistened western slope of the Ural ridge, than on the leeward and relatively dry eastern slope.

**Wind effect** The correlation between the windthrows area and wind effect values is much weaker than one would expect. $R$ is 0.47 for coniferous forests and 0.25 for mixed forests (Fig. 11b). Such weak correlation can be partially explained by coarse spatial resolution of the GMTED-2010 DEM (250 m), which were used to calculate the wind effect. Also, many large windthrows (especially the windthrows in mixed forests) coincide with a flat terrain. The correlation between wind effect and windthrows occurrence is higher in dark-coniferous forests, since this forest type covered large area in the Ural Mountains.

# 5 Conclusion

The main result of the study is the development of the GIS database on large-scale fire- and wind-induced forest disturbances in the Ural region, occurring in 2000–2014. This is one of the first such studies for the territory of Russia, unlike European countries, which have developed long-term data series on natural forest disturbances more than 10 years ago (Schelhaas et al. 2003; Nilsson et al. 2004).

The total area of stand-replacement wildfires and windthrows in the Ural region was estimated at 1.637 million ha, or 1.56% of the entire forested area. The contribution of wildfires and windthrows is 96.4% and 3.6%, respectively. The most fire-affected area is
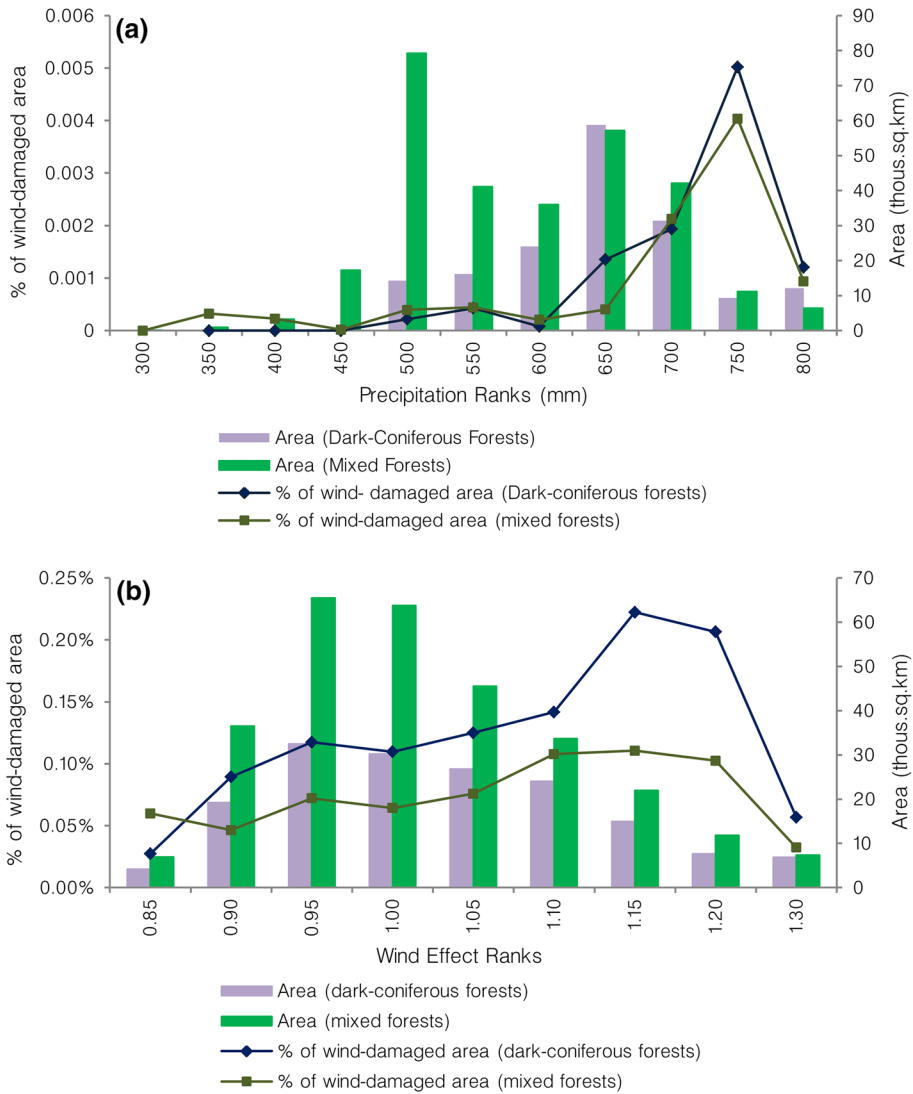
**Fig. 11** Percentage of wind-damaged area versus (**a**) mean annual precipitation, (**b**) wind effect. Bars indicate the proportion of every variable rank in the study area, and lines show the percent of wind-damaged forested area

located behind the Northern Ural ridge, between 64° and 65°N, 63° and 68°E, where the fire scars of 2000–2014 cover 10–14% of the total forested area. The highest windthrows frequency has been observed to the west of the Ural Ridge, near 60°N.

It is important to note that the fire and windthrows size distribution has a strong inequality. A few catastrophic wildfires and windthrows (with an area > 5000 ha) make up 35% of the entire forest losses. The similar size distribution is typical for wildfires in various types of ecosystems (Díaz-Delgado et al. 2004). As for windthrows, such distribution shows that

most of their area is due to infrequent, but destructive squalls (with wind speed $\geq 30$ m/s) and tornadoes, which may occur more often with increasing summer temperatures.

The number of large-scale wildfires and their damaged area has a strong inter-annual variability. In this regard, uncertainty remains in estimating a long-term trend. Six large wildfire outbreaks occurred in the Ural during 2000–2014, and the most severe wildfires happened in 2000, 2010 and 2013. The inter-annual distribution of wildfires has an evident cyclic recurrence, due to the changes in fire–weather conditions in summer. However, it is necessary to obtain a significantly longer data series to confirm this cyclic recurrence and reliably estimate a long-term trend of fire-related forest damage.

As for the windthrows, we may suppose that their frequency and damaged area increase significantly with time during the last 15–20 years. The similar trend was previously found on the entire European Russia for 1985–2012 (Potapov et al. 2015). Severe storms and tornadoes, happened mainly in the Western Ural in 2009, 2010 and 2012, make the main contribution to the increase in forest-damaged area. It is important to note that in a previous study, performed for 1966–1995 (Lassig and Močalov 2000), the positive trend of windthrows area was not identified.

Forests susceptibility to wildfires and windthrows is determined mainly by their species composition. The pine and larch forests are most susceptible to wildfires, especially behind the Ural ridge. Some other environmental variables, such as altitude, slope aspect and mean annual precipitation, also have the statistically significant correlation with the fire-damaged area. The population density has the inverse relationship with the occurrence of large wildfires, since they usually happen in remote low-populated areas. The mean July temperature and lightning frequency do not correlate with the fire-damaged area.

Most of the windthrows occur in mixed and dark-coniferous forests in the Western Ural, between 59° and 62°N. This can be explained both by the wide spread of old-growth dark-coniferous forests, and also by high frequency of strong windstorms and tornadoes in this area (Shikhov and Chernokulsky 2018). The windthrows frequency and wind-damaged area have a strong correlation with annual precipitation, related also to soil moisture. The correlation between the area of windthrows and wind effect parameter, calculated by DEM, is much weaker since the large windthrows are often located in areas with a flat terrain.

The identified patterns of the spatial distribution of wildfires and windthrows can be used to improve forest management. Although windthrows affect a much smaller forest area than wildfires, one should not underestimate their influence, since windthrows frequently occur in the forested areas with intense logging. The old-growth coniferous forests in protected areas (such as Basegi, Vishersky and Pechora-Ilych natural reserves) were also substantially affected by windthrows for the last 15 years. In turn, most of the wildfires occur in the forests of the northeastern Ural, which are less valuable for the regional forest industry.

# References

Afonin AN, Grin SL, Dzubenko NI, Frolov AN (eds) (2008) The agroecological atlas of Russia and neigh-bouring countries: economically significant plants, their pests, diseases and weeds (web-version 2.0). Document freely available on the internet at: http://www.agroatlas.ru

Baranovskiy N, Krechetova S, Belikova M, Perelygin A (2016) WWLLN data cluster analysis methods for lightning-caused forest fires monitoring. Int J Electr Comput Eng 6(6):3112–3120. https://doi.org/10.11591/ijece.v6i6.12780

Bartalev SA, Ershov DV, Isaev AS, Potapov PV, Turubanova SA, Yaroshenko AYu (2004) Russia's for-ests—dominating forest types and their canopy density. Greenpeace Russia and RAS Centre for Forest Ecology and Productivity, Moscow (Map, scale 1:14 000 000)

Bartalev SA, Egorov VA, Loupian EA, Uvarov IA (2007) Multi-year circumpolar assessment of the area burnt on boreal ecosystems using SPOT-VEGETATION. Int J Remote Sens 28(6):1397–1404. https://doi.org/10.1080/01431160600840978

Baumann M, Ozdogan M, Wolter PT, Krylov A, Vladimirova N, Radeloff VC (2014) Landsat remote sensing of forest windfall disturbance. Remote Sens Environ 143:171–179. https://doi.org/10.1016/j.rse.2013.12.020

Bech J, Gayà M, Aran M, Figuerola F, Amaro J, Arús J (2009) Tornado damage analysis of a forest area using site survey observations, radar data and a simple analytical vortex model. Atmos Res 93(1–3):118–130. https://doi.org/10.1016/j.atmosres.2008.10.016

Chuvieco E, Aguado I, Yebra M, Nieto H, Salas J, Martín MP, Vilar L, Martínez J, Martín S, Ibarra P, de la Riva J, Baeza J, Rodríguez F, Molina JR, Herrera MA, Zamora R (2010) Development of a framework for fire risk assessment using remote sensing and geographic information system technologies. Ecol Model 221(1):46–58. https://doi.org/10.1016/j.ecolmodel.2008.11.017

Cohen WB, Spies TA, Alig RJ, Oetter DR, Maiersperger TK, Fiorella M (2002) Characterizing 23 years (1972–95) of stand replacement disturbance in western Oregon forests with Landsat imagery. Ecosys-tems 5(2):122–137. https://doi.org/10.1007/s10021-001-0060-X

De Groot WJ, Cantin AS, Flannigan MD, Soja AJ, Gowman LM, Newbery A (2013) A comparison of Canadian and Russian boreal forest fire regimes. For Ecol Manag 294:23–34. https://doi.org/10.1016/j.foreco.2012.07.033

Degteva SV, Ponomarev VI, Eisenman SW, Dushenkov V (2015) Striking the balance: challenges and per-spectives for the protected areas network in northeastern European Russia. Ambio 44(6):473–490. https://doi.org/10.1007/s13280-015-0636-x

Díaz-Delgado R, Lloret F, Pons X (2004) Spatial patterns of fire occurrence in Catalonia, NE, Spain. Landsc Ecol 19(7):731–745. https://doi.org/10.1007/s10980-005-0183-1

Diffenbaugh NS, Scherer M, Trapp RJ (2013) Robust increases in severe thunderstorm environments in response to greenhouse forcing. Proc Natl Acad Sci USA 110(41):16361–16366. https://doi.org/10.1073/pnas.1307758110

Dmitrieva TG, Peskov BE (2016) Synoptic conditions, nowcasting, and numerical prediction of severe squalls and tornados in Bashkortostan on June 1, 2007 and August 29, 2014. Russ Meteorol Hydrol 41(10):673–682. https://doi.org/10.3103/S1068373916100022

Dyer RC (1988) Remote sensing identification of tornado tracks in Argentina, Brazil, and Paraguay. Photo-gramm Eng Remote Sens 54:1429–1435

Egorov VA, Bartalev SA, Loupian EA, Stytsenko FV (2008) A comparative analysis of the results of the detection of burned areas on the territory of Northern Eurasia according to SPOT-Vegetation and Terra-MODIS data. Curr Probl Remote Sens Earth Space 5(2):292–296 **(in Russian)**

Eliseev AV, Mokhov II, Chernokulsky AV (2014) Influence of ground and peat fires on $CO_2$ emissions into the atmosphere. Dokl Earth Sci 459(2):1565–1569. https://doi.org/10.1134/S1028334X14120034

Fick SE, Hijmans RJ (2017) WorldClim 2: new 1-km spatial resolution climate surfaces for global land areas. Int J Climatol 37(12):4302–4315. https://doi.org/10.1002/joc.5086

Gardiner B, Byrne K, Hale S, Kamimura K, Mitchell SJ, Peltola H, Ruel J-C (2008) A review of mechanis-tic modelling of wind damage risk to forests. Forestry 81(3):447–463. https://doi.org/10.1093/forestry/cpn022

Giglio L, Schroeder W, Justice CO (2016) The collection 6 MODIS active fire detection algorithm and fire products. Remote Sens Environ 178:31–41. https://doi.org/10.1016/j.rse.2016.02.054

Gregow H, Laaksonen A, Alpe ME (2017) Increasing large scale windstorm damage in Western, Central and Northern European forests, 1951–2010. Sci Rep 7, Article 46397. https://doi.org/10.1038/srep46397

Groenemeijer P, Kuhne T (2014) A climatology of tornadoes in Europe: results from the European Severe Weather Database. Mon Weather Rev 142:4775–4790. https://doi.org/10.1175/MWR-D-14-00107.1

Groisman PYa, Sherstyukov BG, Razuvaev VN, Knight RW, Enloe JG, Stroumentova NS, Whitfield PH, Førland E, Hannsen-Bauer I, Tuomenvirta H, Aleksandersson H, Mescherskaya AV, Karl TR (2007) Potential forest fire danger over Northern Eurasia: changes during the 20th century. Global Planet Change 56(3–4):371–386. https://doi.org/10.1016/j.gloplacha.2006.07.029

Hansen MC, Potapov PV, Moore R, Hancher M, Turubanova SA, Tyukavina A, Thau D, Stehman SV, Goetz SJ, Loveland TR, Kommareddy A, Egorov A, Chini L, Justice CO, Townshend JRG (2013) High-resolution global maps of 21st-century forest cover change. Science 342:850–853. https://doi.org/10.1126/science.1244693

Jedlovec GJ, Nair U, Haines SL (2006) Detection of storm damage tracks with EOS data. Weather Forecast 21:249–267. https://doi.org/10.1175/WAF923.1

Koroleva NV, Ershov DV (2012) Estimation of error in determining the forest windfall disturbances area on high spatial resolution space images of LANDSAT-TM. Curr Probl Remote Sens Earth Space 9:80–86 **(in Russian)**

Krylov AM, Malahova EG, Vladimirova NA (2012) Identification and assessment of forest areas damaged by windfalls in 2009–2010 by means of remote sensing. Bull Saint-Petersburg Acad Forest Manag 200:197–207 **(in Russian)**

Krylov A, Potapov P, Loboda T, Tyukavina A, Turubanova S, Hansen MC, McCarty JL (2014) Remote sensing estimates of stand-replacement fires in Russia, 2002–2011. Environ Res Lett 9(10), Article 105007. https://doi.org/10.1088/1748-9326/9/10/105007

Kukavskaya EA, Buryak LV, Shvetsov EG, Conard SG, Kalenskaya OP (2016) The impact of increasing fire frequency on forest transformations in southern Siberia. For Ecol Manag 382:225–235. https://doi.org/10.1016/j.foreco.2016.10.015

Lassig R, Moĉalov SA (2000) Frequency and characteristics of severe storms in the Urals and their influence on the development, structure and management of the boreal forests. For Ecol Manag 135:179–194. https://doi.org/10.1016/S0378-1127(00)00309-1

Loboda T, O'Neal KJ, Csiszar I (2007) Regionally adaptable dNBR-based algorithm for burned area mapping from MODIS data. Remote Sens Environ 109:429–442. https://doi.org/10.1016/j.rse.2007.01.017

Moĉalov SA (2002) Global climate changes and the problems of forest ecology. Bull Ural State Univ 23:48–53 **(in Russian)**

National Atlas of Russia (2008) Borodko AV (ed) Population and economy, vol 3, p 495. Document freely available on the internet at: http://national-atlas.ru/ **(in Russian)**

Nilsson C, Stjernquist I, Bärring L, Schlyter P, Jönsson AM, Samuelsson H (2004) Recorded storm damage in Swedish forests 1901-2000. For Ecol Manag 199(1):165–173. https://doi.org/10.1016/j.foreco.2004.07.031

Panferov O, Doering C, Rauch E, Sogachev A, Ahrends B (2009) Feedbacks of windthrow for Norway spruce and Scots pine stands under changing climate. Environmental Research Letters 4(4):Art. no. 045019. https://doi.org/10.1088/1748-9326/4/4/045019

Potapov P, Turubanova S, Zhuravleva I, Hansen M, Yaroshenko A, Manisha A (2012) Forest cover change within the Russian European North after the Breakdown of Soviet Union (1990–2005). Int J For Res 2012, Article 729614. https://doi.org/10.1155/2012/729614

Potapov PV, Turubanova SA, Tyukavina A, Krylov AM, McCarty JL, Radeloff VC, Hansen MC (2015) Eastern Europe's forest cover dynamics from 1985 to 2012 quantified from the full Landsat archive. Remote Sens Environ 159:28–43. https://doi.org/10.1016/j.rse.2014.11.027

Schelhaas MJ, Nabuurs GJ, Schuck A (2003) Natural disturbances in the European forests in the 19th and 20th centuries. Glob Change Biol 9(11):1620–1633. https://doi.org/10.1046/j.1365-2486.2003.00684.x

Schlyter P, Stjernquist I, Bärring L, Jönsson AM, Nilsson C (2006) Assessment of the impacts of climate change and weather extremes on boreal forests in northern Europe, focusing on Norway spruce. Clim Res 31:75–84. https://doi.org/10.3354/cr031075

Seidl R, Fernandes PM, Fonseca TF, Gillet F, Jönsson AM, Merganiĉová K, Netherer S, Arpaci A, Bontemps J-D, Bugmann H, González-Olabarria JR, Lasch P, Meredieu C, Moreira F, Schelhaas M-J, Mohren F (2011a) Modelling natural disturbances in forest ecosystems: a review. Ecol Model 222(4):903–924. https://doi.org/10.1016/j.ecolmodel.2010.09.040

Seidl R, Schelhaas MJ, Lexer MJ (2011b) Unraveling the drivers of intensifying forest disturbance regimes in Europe. Glob Change Biol 17(9):2842–2852. https://doi.org/10.1111/j.1365-2486.2011.02452.x

Seidl R, Schelhaas M-J, Rammer W, Verkerk PJ (2014) Increasing forest disturbances in Europe and their impact on carbon storage. Nat Clim Change 4:806–810. https://doi.org/10.1038/nclimate2318

Seidl R, Thom D, Kautz M, Martin-Benito D, Peltoniemi M, Vacchiano G, Wild J, Ascoli D, Petr M, Honkaniemi J, Lexer MJ, Trotsiuk V, Mairota P, Svoboda M, Fabrika M, Nagel TA, Reyer CPO

(2017) Forest disturbances under climate change. Nat Clim Change 7(6):395–402. https://doi.org/10.1038/nclimate3303

Shikhov AN, Chernokulsky AV (2018) A satellite-derived climatology of unreported tornadoes in forested regions of northeast Europe. Remote Sens Environ 204:553–567. https://doi.org/10.1016/j.rse.2017.10.002

Shuman JK, Foster AC, Shugart HH, Hoffman-Hall A, Krylov A, Loboda T, Ershov D, Sochilova E (2017) Fire disturbance and climate change: implications for Russian forests. Environ Res Lett 12(3), Article 035003. https://doi.org/10.1088/1748-9326/aa5eed

Soja AJ, Tchebakova NM, French NHF, Flannigan MD, Shugart HH, Stocks BJ, Sukhinin AI, Parfenova EI, Chapin FS III, Jr S (2007) Climate-induced boreal forest change: predictions versus current observations. Global Planet Change 56(3–4):274–296. https://doi.org/10.1016/j.gloplacha.2006.07.028

Stytsenko FV, Bartalev SA, Egorov VA, Loupian EA (2013) Post-fire forest tree mortality assessment method using MODIS satellite data. Curr Probl Remote Sens Earth Space 10:254–266 **(in Russian)**

Virts KS, Wallace JM, Hutchins ML, Holzworth RH (2013) Highlights of a new ground-based, hourly global lightning climatology. Bull Am Meteorol Soc 94(9):1381–1391. https://doi.org/10.1175/BAMS-D-12-00082.1

Vorobiev YuL, Akimov VA, Sokolov YUI (2004) Forest fires in Russia: current state and problems. The Ministry of Emergency of Russia, Moscow **(in Russian)**

Wulder MA, Masek JG, Cohen WB, Loveland TR, Woodcock CE (2012) Opening the archive: how free data has enabled the science and monitoring promise of Landsat. Remote Sens Environ 122:2–10. https://doi.org/10.1016/j.rse.2012.01.010